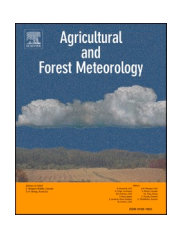
ELSEVIER

Contents lists available at ScienceDirect

Agricultural and Forest Meteorology

journal homepage: www.elsevier.com/locate/agrformet





Changes in crop failures and their predictions with agroclimatic conditions: Analysis based on earth observations and machine learning over global croplands

Tayler Schillerberg, Di Tian

Department of Crop, Soil, and Environmental Sciences, Auburn University, Auburn, Alabama, USA

ARTICLE INFO

Keywords: Crop failure Agroclimatic index Machine learning Prediction Trend Global

ABSTRACT

In this study, we aim to characterize synchronized global crop failures using remote sensing-based products, analyze their predictability and relationships with agroclimatic conditions using machine learning, and identify trends of the most influential agroclimatic indices revealed by machine learning over global croplands. We found that global synchronous crop failures showed strong interannual variability during 1982 to 2016. The most extreme global synchronous crop failure events occurred over 40% of global croplands in the years 2002 (rice and wheat) and 2012 (maize and soy), which had drier and warmer conditions compared to the normal years. Crop failure events can be accurately predicted using machine learning with agroclimatic indices. Of the four crops for both temperate and tropic regions, soy crop failure is most accurately predicted, with an Area Under the Curve (AUC) score of 0.8991 for the temperate region and 0.7892 for the tropics. The AUC score of maize failure in the temperate region is 0.8760, followed by wheat failure (0.8627) and rice failure (0.8025). In the tropics, the remaining crops performed similarly, with AUC scores of 0.7298 (maize), 0.7313 (rice), and 0.7337 (wheat). The machine learning model revealed that growing degree days, last spring frost, first fall frost, growing season precipitation, and optimal field conditions (represented by soil moisture) are the most influential agroclimatic indices, showing various nonlinear relationships with crop failure probabilities. The most influential agroclimatic indices present significant trends on more than 25% of global croplands, showing increasing growing degree days, earlier last spring frost, later first fall frost, while growing season precipitation and optimal field conditions are increasing. Our findings may inform food security predictions, selections of weather index for crop insurance, and climate adaptations.

1. Introduction

Global food security is affected by several factors, including conflict, economic pressures, climate variability and extreme events experienced during and outside of the growing season. Global studies have shown that the growing season precipitation and temperature explain at least one-third of crop yield variability (Lobell and Field, 2007; Ray et al., 2015); extreme precipitation and temperature explain 18-43% of global crop yield anomalies (Goulart et al., 2021; Vogel et al., 2019). According to the FAO, countries that are sensitive to precipitation and temperature extremes and not able to supplement with imports or are reliant on exports from sensitive regions are more likely to become food insecure due to insufficient crop yields, known as crop failures of staple crops (Bren D'Amour et al., 2016; Puma et al., 2015). Currently, most of these

locations are found in Asia, Africa, Latin America, and the Caribbean. These regions would coincide with regions of increased agriculture vulnerabilities if they or a corresponding exporting country were to experience a failure event (Bren D'Amour et al., 2016; Cottrell et al., 2019). Global increases in connectivity allow for areas of surplus to balance out with regions of major yield losses. Synchronized failure events, crop failures occurring across multiple locations in a short time frame, due to extreme events can deplete crop stores, and climate change will result in reductions to crop yield, making it difficult to compensate (Battisti and Naylor, 2009; Powell and Reinhard, 2016; Tigchelaar et al., 2018). Due to climate change, there is an increasing risk of synchronous failure of major crops across the global breadbaskets (Gaupp et al., 2020) and decreased global agricultural productivity growth rate over recent decades (Ortiz-Bobea et al., 2021). Government

E-mail address: tiandi@auburn.edu (D. Tian).

^{*} Corresponding author.

social programs can provide a safety net to reduce the impacts that failure events have on a community allowing individuals to make efforts to adapt to new technologies.

Many key agroecosystem processes take place daily at the local scale as measured by agroclimatic conditions (Trnka et al., 2011), which have strong agricultural significance (Jackson et al., 2021; Kukal and Irmak, 2018; Lobell and Field, 2007) and interests for stakeholders (Matthews et al., 2008). Regional studies using historical observations from Europe, Scotland, and the congenital United States have been performed for growing degree days, frost dates, growing season length, and agroclimate zones (Ceglar et al., 2019; Hatfield et al., 2020; Kukal and Irmak, 2018; Matthews et al., 2008; Trnka et al., 2011) and studies using future projections (Monier et al., 2016; Terando et al., 2012). In the United States, Kukal and Irmak (2018) found a lengthening of the growing season, an increase in growing degree days, and decreases in frost occurrence from 1900 to 2014 for five crops. Similarly, in Europe,

Table 1Description of agroclimatic indices and acronyms. *Denote indices are calculated during the period between planting and harvesting dates.

Agroclimatic Indices (Acronym)	Description	Units	Reference
Last Spring Frost (SpFrost)	Northern Hemisphere: Last frost before July 15 Southern Hemisphere: Last frost before Jan 15	Day of Year (DOY)	(Kukal and Irmak, 2018; Matthews et al., 2008)
First Fall Frost (FallFrost)	Northern Hemisphere: First frost after July 15 Southern Hemisphere: First frost after Jan 15	DOY	(Kukal and Irmak, 2018; Matthews et al., 2008)
Accumulated Frost (FrostDays)	Count of days when $T_{min} < 0^{\circ}C$ between the FallFrost and SpFrost	Days	(Anandhi et al., 2013; Monier et al., 2016)
Climatological Growing Season (GrowSeason)	Number of days between the <i>SpFrost</i> and <i>FallFrost</i> ; can be a year if frost free	Days	(Matthews et al., 2008; Monier et al., 2016)
Start of Field Operations (StFieldOp)	The day when sum of T _{avg} from Jan 1 st (July 1 st) is greater 200°C	DOY	(Matthews et al., 2008; Monier et al., 2016)
Precipitation (Precip)*	$P_{total} = \sum P > 1mm$	mm	(Monier et al., 2016)
Dry Days (<i>DryDays</i>)	$DD = \sum P \le 1mm$	Days	(Monier et al., 2016)
Growing Degree Day (<i>GDD</i>)*	$\begin{split} \frac{T_{max} + T_{min}}{2} - T_{base} \\ T_{base} &= 10^{\circ} \text{C (maize, rice, soy)} \\ T_{base} &= 1^{\circ} \text{C (wheat)} \\ T_{upper} &= 30^{\circ} \text{C (maize, rice, soy)} \\ T_{upper} &= 25^{\circ} \text{C (wheat)} \end{split}$	°C	(Bollero et al., 1996; Kukal and Irmak, 2018; Zhu and Troy, 2018)
Heat Stress Days (HeatDay)*	$\begin{split} &T_{max}>42^{\circ}\text{C (corn)}\\ &T_{max}>35.4^{\circ}\text{C (rice)}\\ &T_{max}>39.4^{\circ}\text{C (soy)}\\ &T_{max}>28.5^{\circ}\text{C (wheat)} \end{split}$	Days	(Monier et al., 2016; Schlenker and Roberts, 2009)(Jackson et al., 2021; Sánchez et al., 2014; Schlenker and Roberts, 2009)
Optimal Field Conditions during: - Planting (FieldCondP) - Mid-season (FieldCondM) - Harvest (FieldCondH)	Days when surface soil water is between 10 to 70% of the maximum water holding capacity & $P_i \le 1$ mm & $P_{i-1} \le 5$ mm during: - Planting: Start of planting to the end of planting range - Mid-Season: Middle of planting to the middle of harvest - Harvest: Start of harvest to the end of harvest to the end of harvest range	Days	(Cooper et al., 1997; Trnka et al., 2011)

Ceglar et al., (2019) found a lengthening of the growing season and increases in temperature-derived indices. Constructed agroclimate zones have decreased in suitability and will continue to do so under future climates. However, these studies only provide regional glimpses and are limited to temperature-based indices, and thresholds in some cases, are not crop-dependent. Globally, Zhu and Troy (2018) analyzed the change in several different agroclimate indices for maize, rice, soy, and wheat growing seasons. In their trends, they find an inflection point occurring around 1980, where temperature-based indices began to increase rapidly globally, while precipitation-based trends showed regional distributions.

Future conditions and climate extremes are expected to deteriorate growing season conditions increasing yield volatility (Mangani et al., 2018; Nóia Júnior et al., 2021; Powell and Reinhard, 2016); however, yield declines may occur earlier than expected (Jägermeyr et al., 2021). Monthly precipitation and temperature are among the most common climate variables to be considered when estimating climate impacts on crop yields. Other climate variables like solar radiation, soil moisture, evaporative demand, and diurnal temperature range have regional relevance in determining crop yields (Brown, 2013; Gaupp et al., 2020; Goulart et al., 2021; Lobell et al., 2013). Using monthly temperature and precipitation information, both Lobell and Field (2007) and Ray et al. (2015) suggested that globally at least one-third of yield variability is due to the weather experienced during the growing season. Using aggregated climate information at the monthly level, Ortiz-Bobea et al. (2021) showed that agriculture productivity has slowed due to anthropogenic climate change in recent decades. Regionally in the United States, Li et al. (2019) showed that extreme temperature and precipitation values could affect maize yield. Using high precipitation as an example, they also discussed how some crop models might be unable to capture the complete non-linear response of yield to precipitation. More recent studies (Goulart et al., 2021; Vogel et al., 2019) have used machine learning to explore daily and monthly climate data impacts on yield regionally and globally. Vogel et al. (2019) found a stronger association with temperature and yield anomalies at the national level over the globe, while Goulart et al. (2021) indicated that temperature, precipitation, and the diurnal temperature range contributed to crop failure in the United States Midwest. Gaupp et al. (2020) found an increased risk of high-production regions, breadbaskets, failing of maize, soy, and wheat when comparing two time periods from 1967 to 2012 using a vine copula approach. A staple crop failure event in a high-production region may result in unrest and food insecurity in another that depends on imports (Battisti and Naylor, 2009; Cottrell et al., 2019; FAO et al., 2021; Lau et al., 2012; Nóia Júnior et al., 2021; Wegren, 2011), suggesting that a global assessment of crop failures and their predictability using agroclimate indices is needed beyond the regional or national level.

In this study, we aim to characterize synchronized global crop failures using remote sensing-based products, analyze their predictability and relationships with agroclimatic conditions using machine learning, and identify trends of the most significant agroclimatic indices over global croplands. The key questions posed were: over the past decades, from 1982 to 2016, what is the spatiotemporal distribution of synchronized maize, rice, soy, and wheat crop failures over global croplands revealed by remote sensing-based products? How well can crop failures be predicted by machine learning with agroclimatic indices? What are the responsive relationships of remote sensing-characterized crop failures to changes in agroclimatic indices as revealed by machine learning? How have the impactful agroclimatic indices changed over the past decades? We chose four crops because maize, rice, and wheat are the three main cereal crops accounting for 90% of the production (Erenstein et al., 2021; FAO, 2021; FAO et al., 2021), and soy accounts for 60% and 70% of oilseed and meal protein (USDA Foreign Agricultural Service, 2021). Our study considers 11 agroclimatic indices that have strong agricultural significance and stakeholder interests, many of which have been neglected in previous global-scale studies. In addition, developing

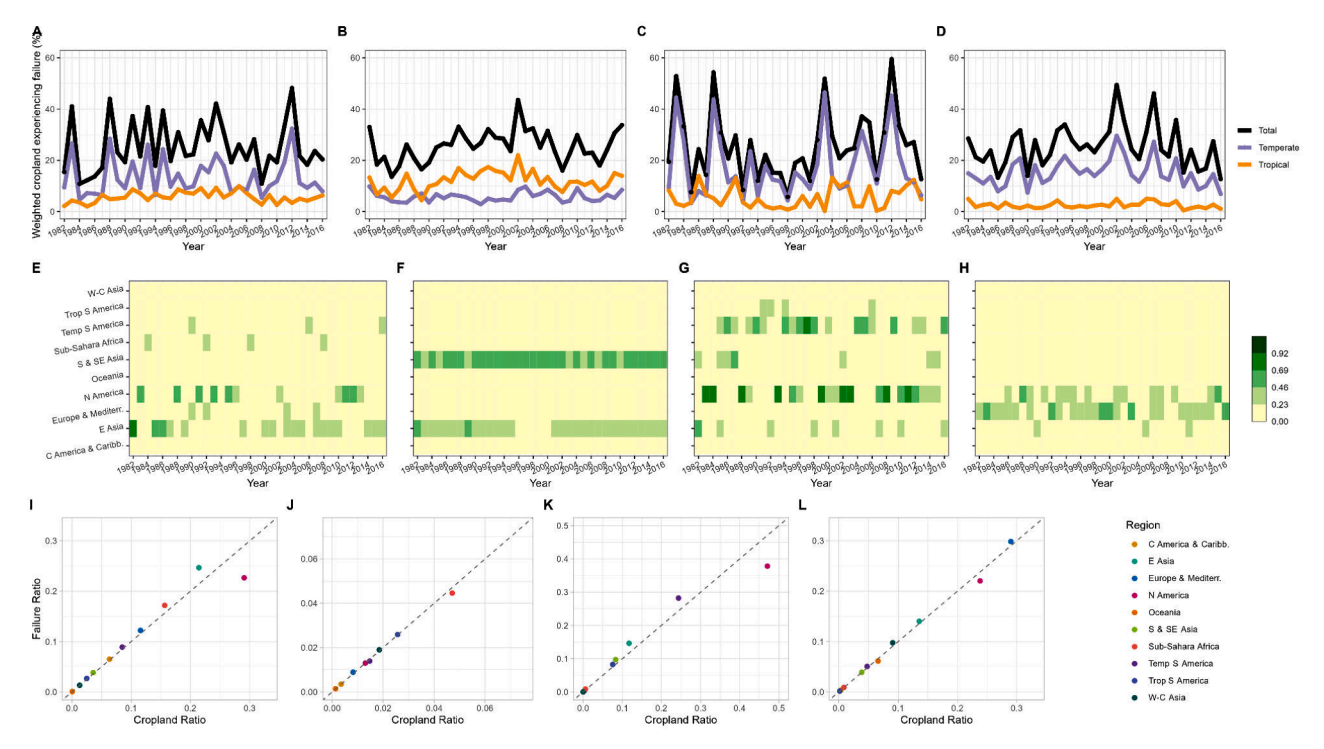


Fig. 1. (A-D) The annual percentage of global cropland experiencing synchronous crop failure with contributions from temperate and tropical regions. (E-H) Individual region's contribution to global synchronous failure during 1982-2016. (I-L) The contribution of regional crop failure to global crop failure versus the contribution of regional cropland to global cropland. For each row, from left to right, maize (A, E, I), rice (B, F, J), soy (C, G, K), and wheat (D, H, L).

a machine learning-based approach to predicting and analyzing the crop failure is rarely investigated in previous work. This work can potentially inform food security predictions, selections of weather index for crop insurance, and global climate adaptations.

2. Data & methods

2.1. Climate and crop data

Daily maximum and minimum temperature and precipitation during 1981-2017 were retrieved from the National Aeronautics and Space Administration (NASA) Langley Research Center (LaRC) POWER Project (https://power.larc.nasa.gov/), which is available at a 0.5° by 0.5° resolution. Daily surface (0-10cm) soil moisture from 1981-2017 was obtained from GLEAM v3.3a (Martens et al., 2017; Miralles et al., 2011) at 0.25° resolution and aggregated into 0.5°, to be consistent with the other datasets used in this study. Annual yield data for four staple crops (maize, rice, soy, and wheat) was obtained from the Global Dataset of Historic Yield (Iizumi, 2019; Iizumi and Sakai, 2020) during 1981-2016 at a 0.5° resolution, which is a hybrid data by combining agricultural census statistics and satellite remote sensing. (Sacks et al., 2010) provided 0.5° resolution of planting and harvesting dates for several crops, which has been widely utilized in crop yield analysis (Iizumi and Sakai, 2020; Ray et al., 2015; Vogel et al., 2019). Main season planting and harvesting dates of maize, rice, soy, spring, and winter wheat were used to calculate crop-dependent agroclimatic conditions at each grid point and growing season congruent with regional agricultural calendars. Cropland masks are created using planting, harvesting, and EarthStat crop production data (Monfreda et al., 2008) to limit analysis to cropland regions devoted to maize, rice, soy, or wheat. EarthStat production data provides locations of high and low crop production globally circa 2000. Cropland weights were created for the aggregated cells using EarthStat fractional harvested area. Give more value to cells with larger production areas devoted to crop production than regions with smaller production amounts, reducing the impact of large land masses with less

dense agriculture production. Regions with smaller weights and dependent on imports may be more sensitive to teleconnection supply shocks (Bren D'Amour et al., 2016; Cottrell et al., 2019). Global cropland was divided into ten regions (Supplementary Fig. 1). Yield data is linearly detrended using the M estimator, which is robust against vertical outliers and performs similarly to ordinary least squares in heteroscedasticity and skewed distributions (Finger, 2013). Detrending minimizes the effects of advances in management practices and technologies. Detrended yields were then divided into quartiles, in which the lowest quartile was defined as crop failure (Gaupp et al., 2020; Schillerberg and Tian, 2020).

2.2. Agroclimatic indices

Twelve agroclimatic indices (Table 1) were calculated for each growing season during 1982-2016 to characterize agroclimatic conditions for their significance in agriculture (Kukal and Irmak, 2018; Monier et al., 2016; Trnka et al., 2011) and salience among stakeholders (Gowda et al., 2018; Matthews et al., 2008). The agroclimatic indices were calculated at each grid point over global croplands except for several unique instances, such as tropics where frost occurrences are rare. Planting and harvesting dates determine crop-specific growing seasons. For example, Precip, DryDays, GDD, and HeatDay were calculated from the planting season to the end of the harvest season as specified in (Sacks et al., 2010) for each grid cell. FieldCondP (Field-CondH) is calculated from the start of planting (harvest) to the end of planting (harvest) and FieldCondM from the middle of planting to the middle of harvest, allowing the capture of early and late-season crop planting. In addition, time series of the impactful agroclimatic indices from 1982-2016 were analyzed using the Mann-Kendall trend test for each grid point over global croplands. Grid cells with more than 50% missing data were removed before the analysis. Mann-Kendall is a non-parametric test to determine if a monatomic increasing or decreasing trend is present (Wilks, 2011). A trend is considered as significant when the p-value is smaller than 0.10.

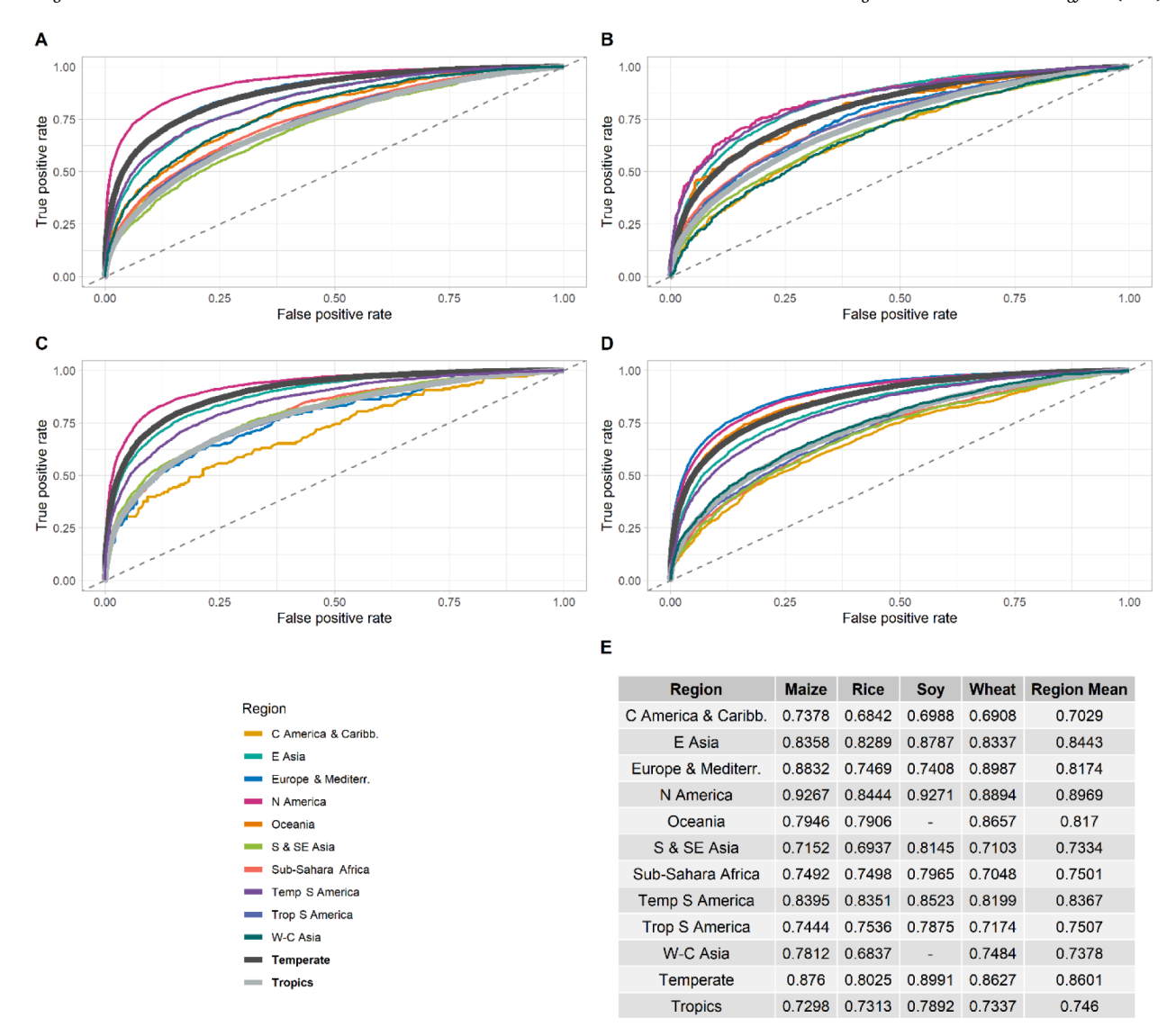


Fig. 2. Performance of the random forest models for predicting crop failure occurrence based on agroclimatic indices for the 10 individual regions, and temperate and tropic regions. (A-D) ROC curves for Maize, rice, soy, and wheat, (E) AUC scores. "—" indicate the data is not available for that region.

2.3. Random forest

Random forest is a non-parametric classification and regression tree analysis method based on ensemble machine learning algorithms. Random forest constructs multiple decision trees composed of bootstrapped resamples of the training data (Breiman, 2001; Liaw and Wiener, 2018). The random forest has been utilized in recent studies of climate impacts on agriculture in different regions (Goulart et al., 2021; Schierhorn et al., 2021; Schillerberg et al., 2019; Schillerberg and Tian, 2020; Vogel et al., 2019) and found to be more effective than commonly used multiple linear regression for predicting crop yields (Jeong et al., 2016; Leng and Hall, 2020). We construct random forest models for each of the ten crop production regions as well as two additional models, one for the temperate regions (the areas experiencing more than one frost a year) and the second for the tropics (regions not experiencing frost) (Supplementary Fig. 1). We performed cross-validation using a random 70/30% split of the data for training and testing with 500 runs. Specifically, we withheld 30% of the data randomly sampled from all the pixels and years in a region for model testing and used the rest 70% for model training. The large spatial extent of each region provides a large sample size covering a variety of agroclimate conditions and crop failure or non-failure conditions. Since the training and testing data are

randomly sampled in space and time, it eliminated spatial and temporal correlations between the training and testing datasets. The performance of the random forest models was evaluated using the relative operating characteristic (ROC) curves. ROC curves represent the relationship between true- and false-positive rates at different thresholds. A ROC curve is assigned a score by integrating the area under the curve (AUC) and considers all possible threshold values. An AUC score of 0.5 represents a model with the same true- and false-positive rate for every threshold, providing no more information than a coin flip, and an AUC score of 1 represents a model of perfect predictors. Partial Dependency plots (PDP) show the marginal effect of one or two features on the predicted outcome of the random forest model. We constructed PDP for each random forest model to visualize dependence relations between agroclimatic conditions (predictors) and crop failures (response variable). PDP is a global method that considers all instances between the response variable and predictors while all remaining predictor variables are held constant (Molnar, 2019). A 95% confidence interval was computed for PDPs based on the 500 cross-validation runs to quantify the uncertainty associated with the estimation. Since thousands of samples are used for constructing each random forest model, the 95% confidence interval are generally very small, suggesting robust model estimations.

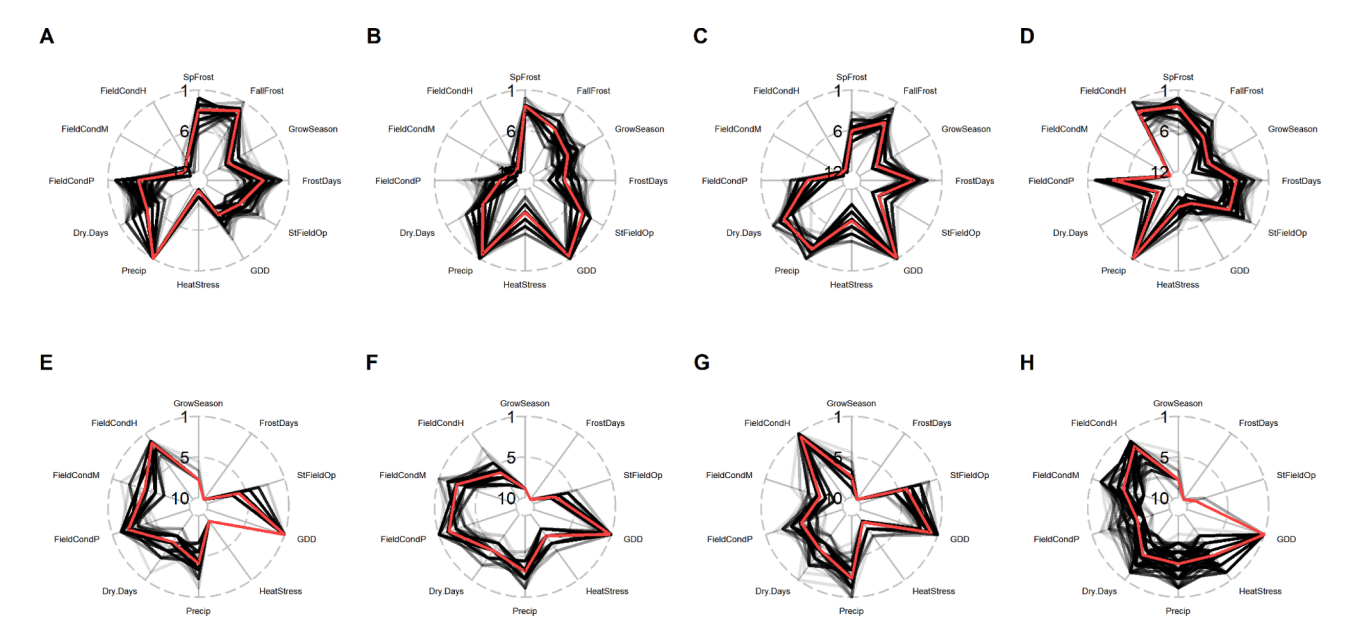


Fig. 3. Agroclimate variable importance ranking of 500 cross validation runs (grey) and the average (red) to determine crop failure of different crops, from left to right: maize (A, E), rice (B, F), soy (C, G), and wheat (D, H) for the temperate (top row) and tropic (bottom row) region. Darker lines indicate more agreement between model runs. Distance from the center indicates variable importance, more important variables are further away from the center with the least important variables closer to the center.

3. Results

3.1. Distributions of synchronous global crop failures

Here we refer crop failures occurring across different locations in the same year as synchronous crop failures. We present distributions of synchronous crop failures for maize, rice, soy, and wheat over the globe from 1982 to 2016 and over each region (Fig. 1). The results indicate no clear trend in synchronous global crop failures for either tropic or temperature regions, while the interannual variability is very strong, ranging from less than 5% to 60% globally (Fig. 1A-D). The most extensive synchronous crop failure events occurred in the years 2002 (rice and wheat) and 2012 (maize and soy), with over 40% of weighted global cropland experiencing failures over those years. We further examine the contribution of regional cropland to global cropland experiencing failure in each of the ten individual regions (Fig. 1E-H). There are a few regions where the contributions are particularly large in most of the years, including North America for maize and soy failures, South and Southeast Asia for rice failures, East Asia for rice and wheat failures, temperate South America for soy failures. On average, the contributions of different regions to global crop failures are generally proportional to their contributions to global croplands (Fig. 1I-L). However, there are a few exceptions where the regions contribute less to global cropland but more to global crop failures (Fig. 1I-L), which include East Asia and Sub-Sahara Africa for maize (Fig. 1I), Temperate South America and East Asia for soy (Fig. 1K), and Europe and the Mediterranean for wheat (Fig. 1L). These regions tend to be more susceptible to failures of specific crops than the other regions.

3.2. Predicting crop failure occurrence using agroclimatic indices

We constructed random forest models to predict crop failure occurrence for each crop using the agroclimatic indices (Table 1) over the temperate region, the tropics region, and each of the ten crop production regions. The models were cross validated, meaning the data used for model validation was excluded from model training. On average, the random forest models with agroclimatic indices can accurately predict crop failures on the validation data, with an AUC score of 0.7460 for the tropic region and 0.8601 for the temperate region (Fig. 2). Of the four

crops for both regions, soy crop failure is most accurately predicted, with an AUC score of 0.8991 for the temperate region and 0.7892 for the tropics. The AUC score of maize failure in the temperate region is 0.8760, followed by wheat failure (0.8627) and rice failure (0.8025). In the tropics, the remaining crops models performed similarly, with AUC scores of 0.7298 (maize), 0.7313 (rice), and 0.7337 (wheat).

Regarding the regional patterns, the North American region has the highest AUC values for maize (0.9267) and soy (0.9271). The AUC values for rice (0.8444) and wheat (0.8894) in North America are close to those in Temperate South America (rice, AUC value 0.8351) and Europe and Mediterranean (wheat, AUC value 0.8987) regions. Central America and the Caribbean is the lowest-performing region, with an AUC value of 0.6842 for rice and 0.6908 for wheat. Across crops, rice has the lowest performance, possibly due to its varied management practices and heavy reliance on irrigation, which counteracts the effects of low precipitation, heat stress, and dry days (Ceglar et al., 2017; Tack et al., 2017; Zaveri and Lobell, 2019). These results suggested that agroclimatic indices can accurately predict crop failures, suggesting that crop failures have been strongly influenced by agroclimatic changes, and the models based on the agroclimatic indices can be potentially useful for crop failure early warning.

3.3. The relative importance of agroclimatic indices

The random forest models with cross-validation run for each region allow us to quantify the relative importance of agroclimatic indices in estimating crop failure occurrences. Fig. 3 shows several influential variables ranked consistently high in almost all the 500 cross-validation runs. In the temperate region, these variables include the growing season precipitation (*Precip*), fall frost (*FallFrost*) for maize failures, *Precip*, growing degree days (*GDD*) and spring frost (*SpFrost*) for rice failures, *Precip*, *GDD* and the number of dry days (*DryDays*) for soy failures, and *Precip* and days of optimal field conditions during harvest (*FieldCondH*) for wheat failures. In the tropics, they include *GDD*, *FieldCondH* and optimal field conditions during planting (*FieldCondP*) for maize failures, *GDD*, *FieldCondP*, and optimal field conditions during mid-season (*FieldCondM*) for rice failures, *GDD* and *FieldCondH* for soy failures, and *GDD* for wheat failures. While the ranking of variable importance from regional models shows variations among different regions and

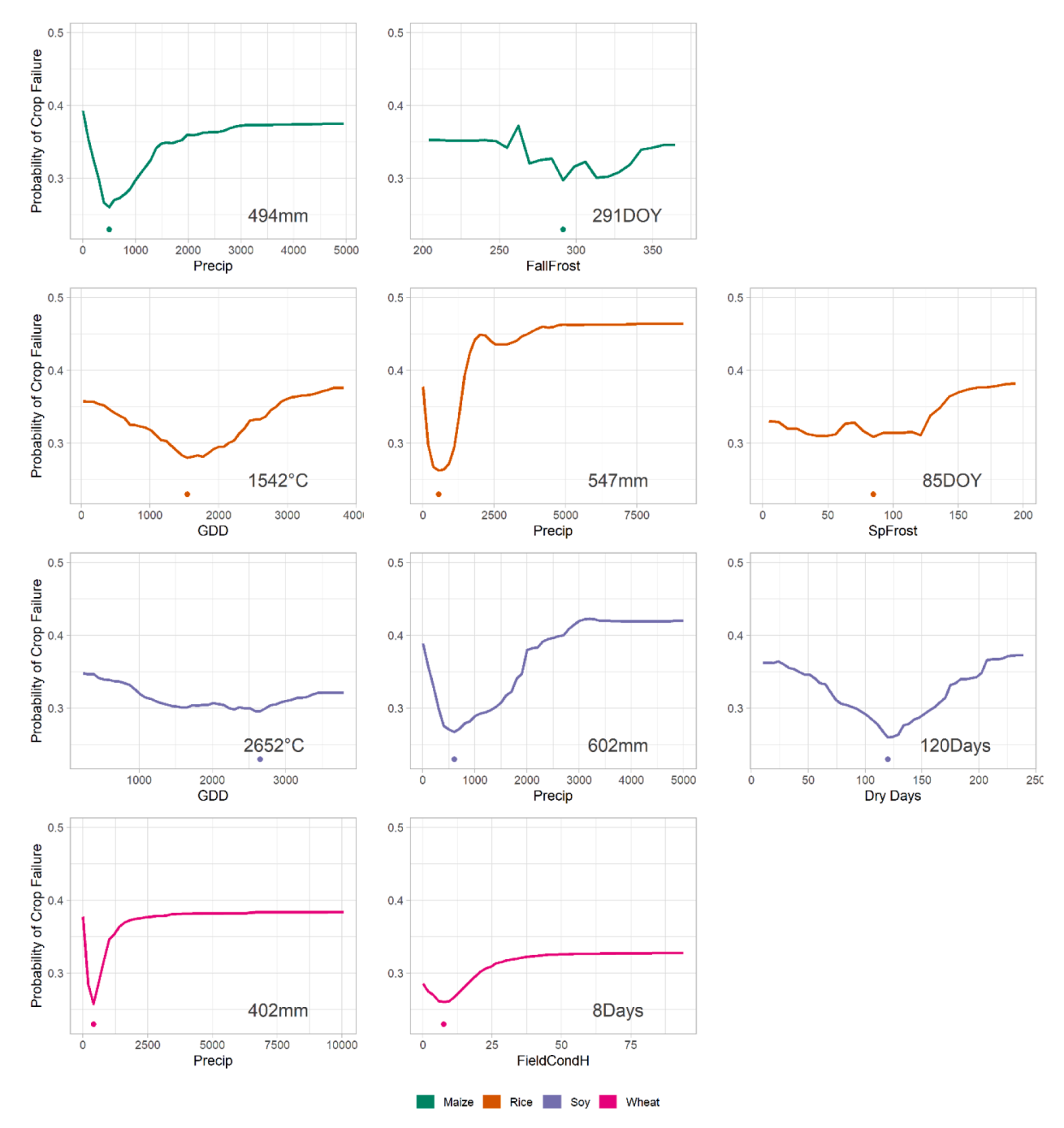


Fig. 4. Partial dependency plot showing the response of crop failure probability to the most influential agroclimatic indices identified by the random forest models in the temperature region. Rows represent each crop, from top to bottom: maize (A-B), rice (C-E), soy (F-H), and wheat (I-J). The dot and text in the figure represent the optimal agroclimatic condition with minimum crop failure probability. The optimal conditions for each of the ten individual regions are presented in the Supplementary Fig. 3.

crops (Supplementary Fig. 2), it identifies similar influential agroclimatic indices as the global analysis by temperate region and tropics.

3.4. Response of crop failure to changes in agroclimatic conditions

Here we present the Partial Dependency Plots (PDP) of the random forest models to examine the response of crop failures to the changes of the influential agroclimatic indices identified in the last section for each crop in the temperate region (Fig. 4) and tropics (Fig. 5), respectively, with conditions for minimum crop failures probabilities noted in the plots. In the temperate region, crop failures of all four crops are responsive to the *Precip* changes. The increase in crop failure probability

due to excessive *Precip* is almost the same as due to deficient *Precip* and reaches the maximum when *Precip* exceeds approximately 2000mm, despite the higher reoccurrence of deficient *Precip* in the historical record. For rice and soy, the probability of crop failures gradually increased with the addition or reduction of *GDD*, higher *GDD* is associated with higher failure risks. For rice failures, late *SpFrost* (>85 day of year, DOY) or early *FallFrost* (<291 DOY) dramatically increases the failure probabilities. As an influential variable for soy failure, shifting from optimum *DryDays* (120 days) gradually increases the probability of soy failures. Greater or smaller than 8-day *FieldCondH* increased wheat failure probabilities, while higher *FieldCondH* is associated with much higher risks than lower ones. In the tropics, crop failures of all four crops

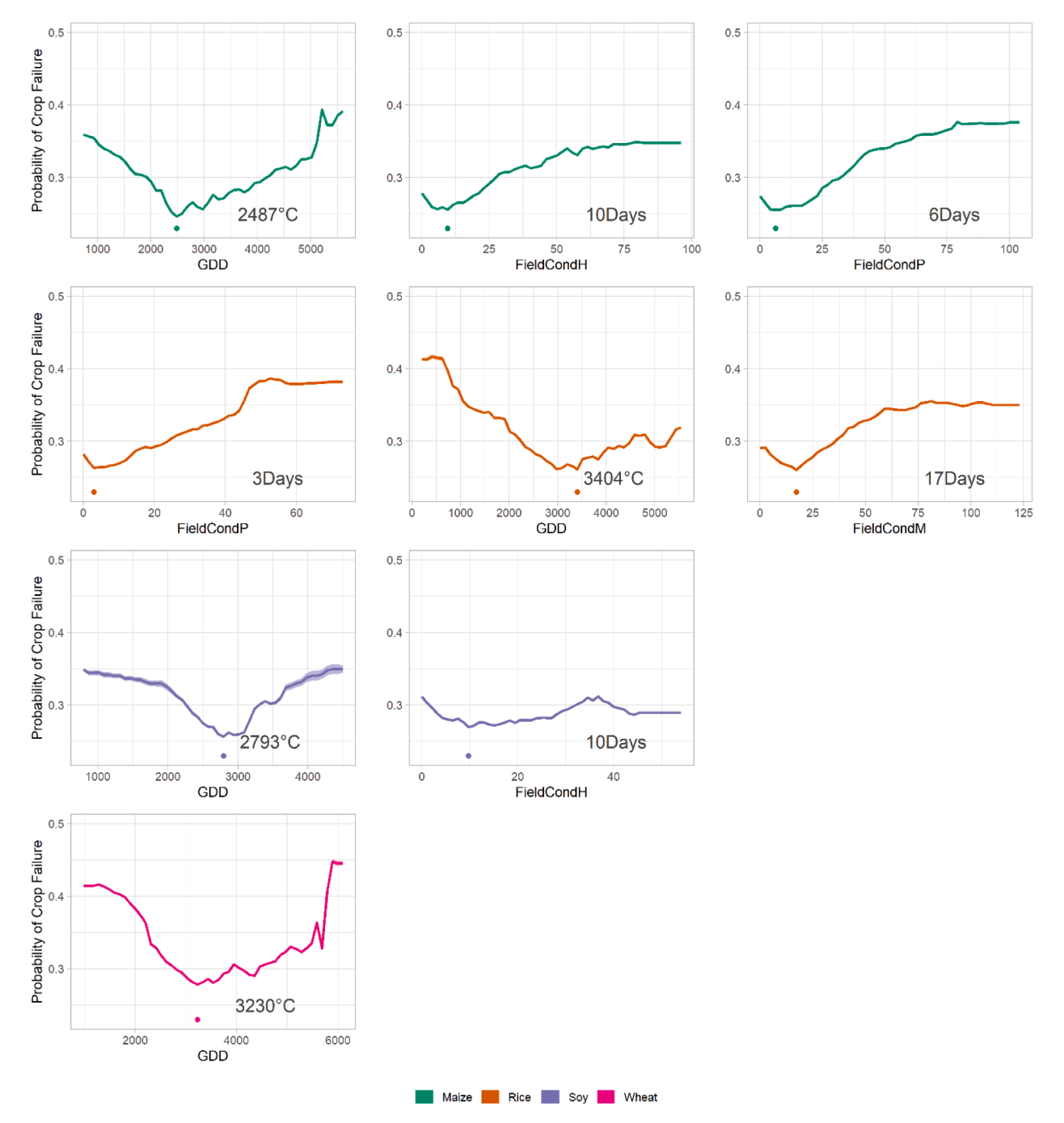


Fig. 5. Partial dependency plot showing the response of crop failure probability to the most influential agroclimatic indices identified by the random forest models in the tropic region. Rows represent each crop, from top to bottom: maize (A-C), rice (D-F), soy (G-H), and wheat (I). The dot and text in the figure represent the optimal agroclimatic condition with minimum crop failure probability. The optimal conditions for each of the ten individual regions are presented in the Supplementary Fig. 3.

are very responsive to the changes in *GDD*. Either increasing or decreasing *GDD* can gradually increase the probability of crop failures up to 0.45. The increasing or decreasing of *FieldCondH* and *FieldCondP* is associated with increased maize failure risks, with increased values associated with more dramatically increased failure probability compared to the decreased values. The response of rice failures to *FieldCondP* is similar to maize failures. While *FieldCondM* shows a similar responsive relationship as *FieldCondP* for rice failures. For soy failures, the responsive relationship with *FieldCondH* is similar to maize or rice failures.

It is worth noting that the optimal *GDDs* with minimum failure probability are maize 2487°C, rice 3404°C, soy 2793°C, wheat 3230°C

for the tropics, which are much higher than temperate region, while the *Precip* associated with the minimum crop failure probability are maize 494mm, rice 547mm, soy 602mm, and wheat 402mm for the temperate region, much lower than the tropics. The agroclimatic conditions with minimum crop failure probabilities identified for each of the individual regions are presented in Supplementary Fig. 3.

3.5. Trends of agroclimatic conditions of significance to crop failures

We examined the percentage of regional cropland experiencing significant trends (p-value < 0.10) in the identified influential agroclimatic indices (Fig. 6) and whether they are increasing or decreasing

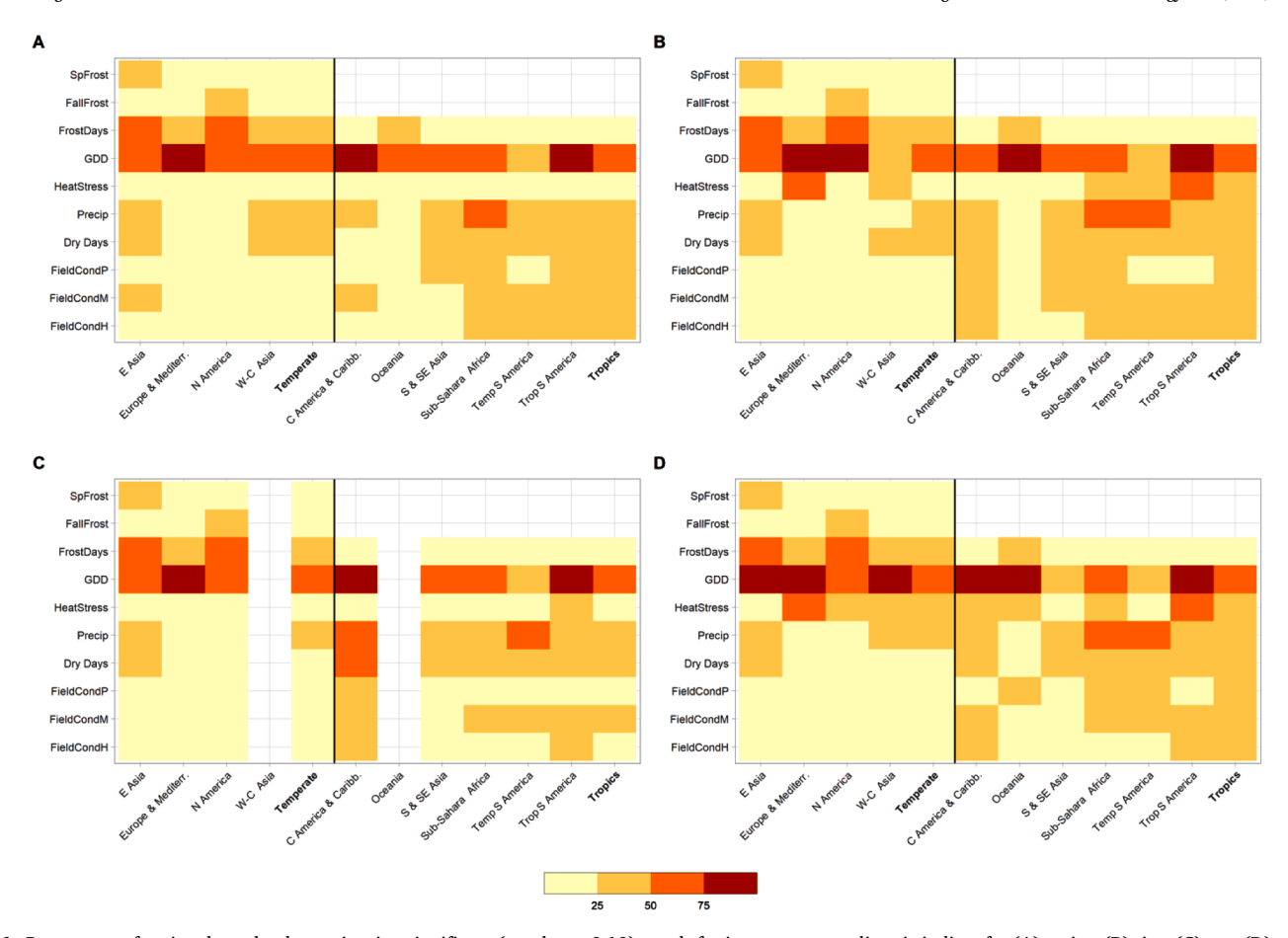


Fig. 6. Percentage of regional cropland experiencing significant (p-value < 0.10) trends for important agroclimatic indices for (A) maize, (B) rice, (C) soy, (D) wheat. Percentage of area showing increasing or decreasing trends are presented in the supplementary Fig. 4.

(Supplementary Figs. 4 and 5). We can see that more than 25% of tropical croplands are experiencing significant trends in *GDD*, *HeatDay*, *Precip*, *DryDays*, *FieldCondP*, *FieldCondM*, or *FieldCondH* for almost all crops, while more than 25% of temperate croplands are experiencing significant trends in *FrostDays*, *GDD*, *Precip*, and *DryDays* for maize and rice, *FrostDays*, *GDD*, and *Precip* for soy, and *FrostDays*, *GDD*, *HeatDay*, and *Precip* for wheat. Quite a few regions are experiencing significant agroclimatic trends in more than 50% of their croplands, including decreasing *FrostDays* in 100% East Asia and North America for all four crops, increasing *GDD* in almost all regions for all crops, decreasing *HeatDay* in Europe and the Mediterranean and Tropic South America for both rice and wheat, *Precip* in Sub-Saharan Africa for maize, rice, and wheat and in Temperature South America for soy, and *DryDays* in Central America and Caribbean. All these indices with significant trends are among the most influential indices identified in the last sections.

Globally, *GDD* trends are consistently increasing, while *Precip* trends show strong variations with increasing and decreasing trends mostly occurring in the temperate and tropic regions, respectively (Supplementary Fig. 4). These increasing warming trends are similar for all the temperature-based indices, as reflected in increasing *GDD* and *HeatDay*, decreasing *FrostDays*, earlier *SpFrost*, and later *FallFrost*, and moisture-based indices, as reflected in increasing or decreasing *Precip*, *DryDays*, *FieldCondP*, *FieldCondM*, or *FieldCondH*, while the percentage of significant increasing or decreasing trends varied by regions (Supplementary Fig. 5).

We examined the conditions of the most influential agroclimatic indices on the failure croplands during the years with extreme global crop failure events, including maize 2012, rice 2002, soy 2012, and wheat 2002 (Figs. 7 and 8). While there are slight spatial variations, the results generally show dryer and warmer conditions during those

extreme years compared to the optimal conditions in both tropics and temperate region. Given the increasing trends, the temperature-based indices are generally shifting towards the conditions of extreme crop failure years for both temperature and tropic regions. While the moisture trends are increasing, not changing towards the conditions of extreme years, regions experiencing significant trends (Supplementary Fig. 5) may face increasing risks of crop failures through excessive moisture or dryness (Fig. 4) compared with the regions with no significant moisture trends. In Figs. 9 and 10, we further show that, at each location, whether the trends point toward more detrimental or beneficial conditions by finding the difference between the average agroclimate indices over 1982 to 2016 and the average value of the agroclimate indices when crop failure occurs considering the direction of the significant trend at that location. Specifically, the current trends are trending toward more detrimental conditions if decreasing the distance between the agroclimate mean and the agroclimate condition when failures occurred, while are trending toward more beneficial conditions if increasing the distance between the agroclimate mean and the agroclimate condition when failures occurred. There are varied beneficial and detrimental trends in the temperate and tropics region throughout the regions when looking at the agroclimate indices. Precip and precipitation-derived agroclimate indices have strong spatial variation present. Increases in Precip (Supplemental Fig. 5) increase beneficial conditions for maize in temperate regions of northern North America but harmful conditions in Midwest North America and China (Fig. 9). Temperature-derived variables, like GDD, FallFrost, and SpFrost, have mostly showed consistent trends in space, while also experiencing regions of beneficial and detrimental condition trends (Figs. 9 and 10).

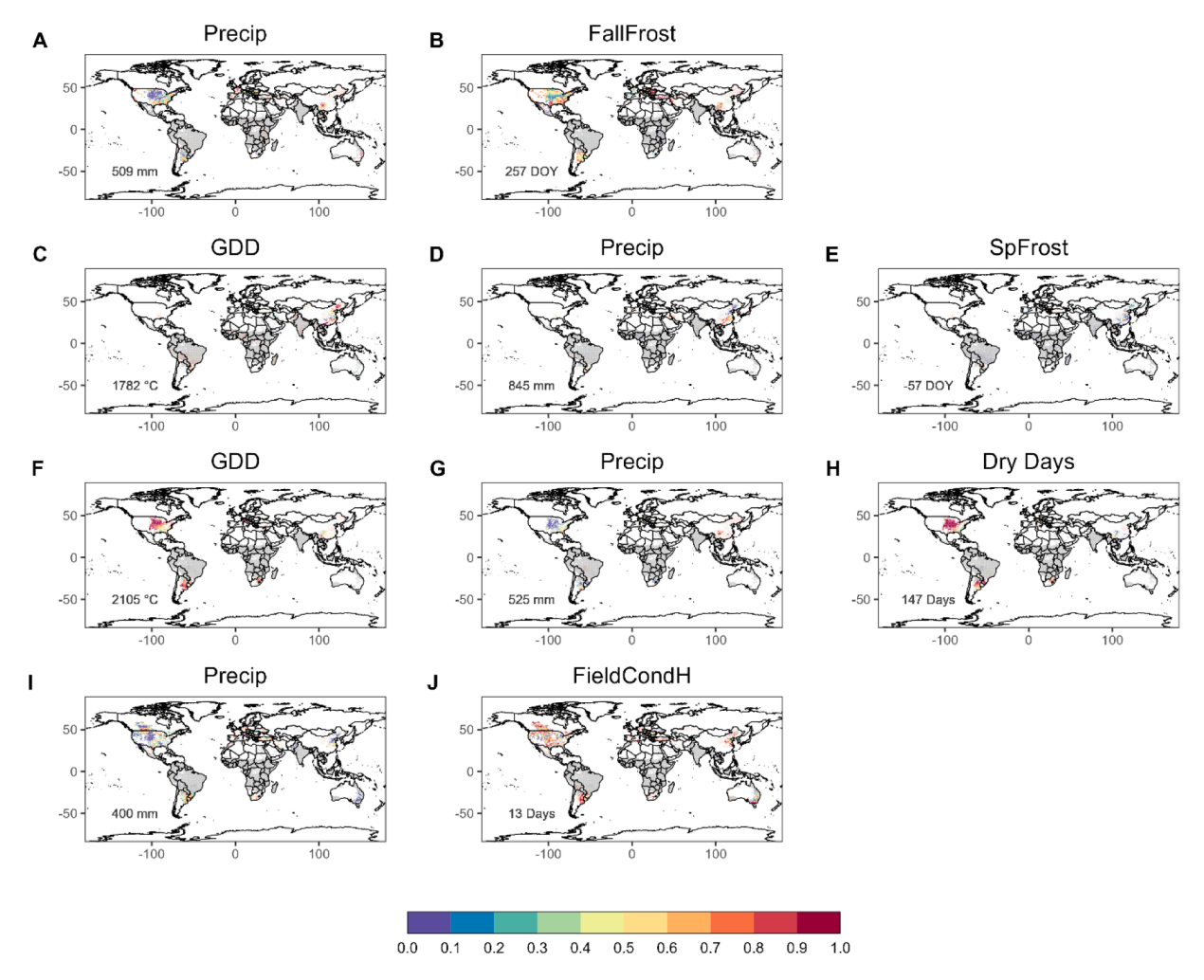


Fig. 7. The most influential agroclimatic indices in the temperate region on global croplands experiencing failures during extreme years for maize 2012 (A-B), rice 2002 (C-E), soy 2012 (F-H), and wheat 2002 (I-J) (from top row to bottom row). The color shows the percentile value for each pixel; the text shows the average of actual value. Grey areas are the tropic region.

4. Discussion

In the previous studies, Gaupp et al. (2020) have found an increase in synchronous breadbasket failure, while Mehrabi and Ramankutty (2019) have found trends in synchronized crop production have declined. Globally across temporal and tropical regions, we find no significant global synchronized crop failure trends from 1982 to 2016 for the four staple crops. We also identify several years of high (>40% global cropland) synchronous global crop failures (2002 for rice and wheat, 2012 for maize and soy), consistent with previous literature (Gaupp et al., 2020; Goulart et al., 2021; Mehrabi and Ramankutty, 2019). Synchronous crop failure events are influenced by large-scale oscillations such as ENSO, affecting nearly 20% of maize production (Anderson et al., 2019), which may have influenced crop failure of rice and wheat in 2002, the year experiencing moderate El Nino. We note several regions which are identified as contributing more to global crop failure than their contributions to global cropland after accounting for cropland weight, including East Asia and Sub-Sahara Africa for maize, Temperate South America for soy, and Europe and the Mediterranean for wheat. Several of these regions coincide with regions of higher yield variability (Iizumi and Ramankutty, 2016). For example, southeast Asia is a known breadbasket for rice but faces high production shocks (Cottrell et al., 2019) and results in food supply shocks in regions, western Africa and Malaysia, dependent on rice from this region (Bren D'Amour et al., 2016). Future climatic warming will increase crop variability,

increasing the probability of synchronous failure globally (Gaupp et al., 2019; Tigchelaar et al., 2018), which may result in more countries relying more heavily on stressed grain stores and exports, challenging countries to balance increased import costs and feeding their populations.

Consistent with Schlenker and Roberts (2009), we find non-linear effects from temperature; however, we also find that these non-linear effects exist in the other agroclimate indices and are influential on crop failure probabilities beyond temperature. This study identified GDD and Precip (acronyms and shortened agroclimate indices can be found in Table 1) as influential on crop failures, confirming previous findings that Precip and GDD are the most common climate variables to explain crop yield variations, explaining up to 60% of variability regionally and one-third of global variability (Lobell et al., 2012; Lobell and Field, 2007; Ray et al., 2015; Tigchelaar et al., 2018). Growing season temperature has long been used to predict yields (Lobell and Field, 2007; Tigchelaar et al., 2018) as it is an indicator of the thermal time required for growth and the effects of temperature explored in depth to the vegetative and reproductive periods (Asseng et al., 2015; Muchow et al., 1990; Peltonen-Sainio et al., 2011). Too much or too little Precip can negatively affect yield since precipitation deficit during the reproductive period impacts tasseling and ear formation in maize, leading to reduced yield (Çakir, 2004; Kamara et al., 2003; Song et al., 2018). Excessive rainfall can reduce yields through waterlogging, ponding, and flooding, causing root damage and nitrogen deficiency, comparable to the

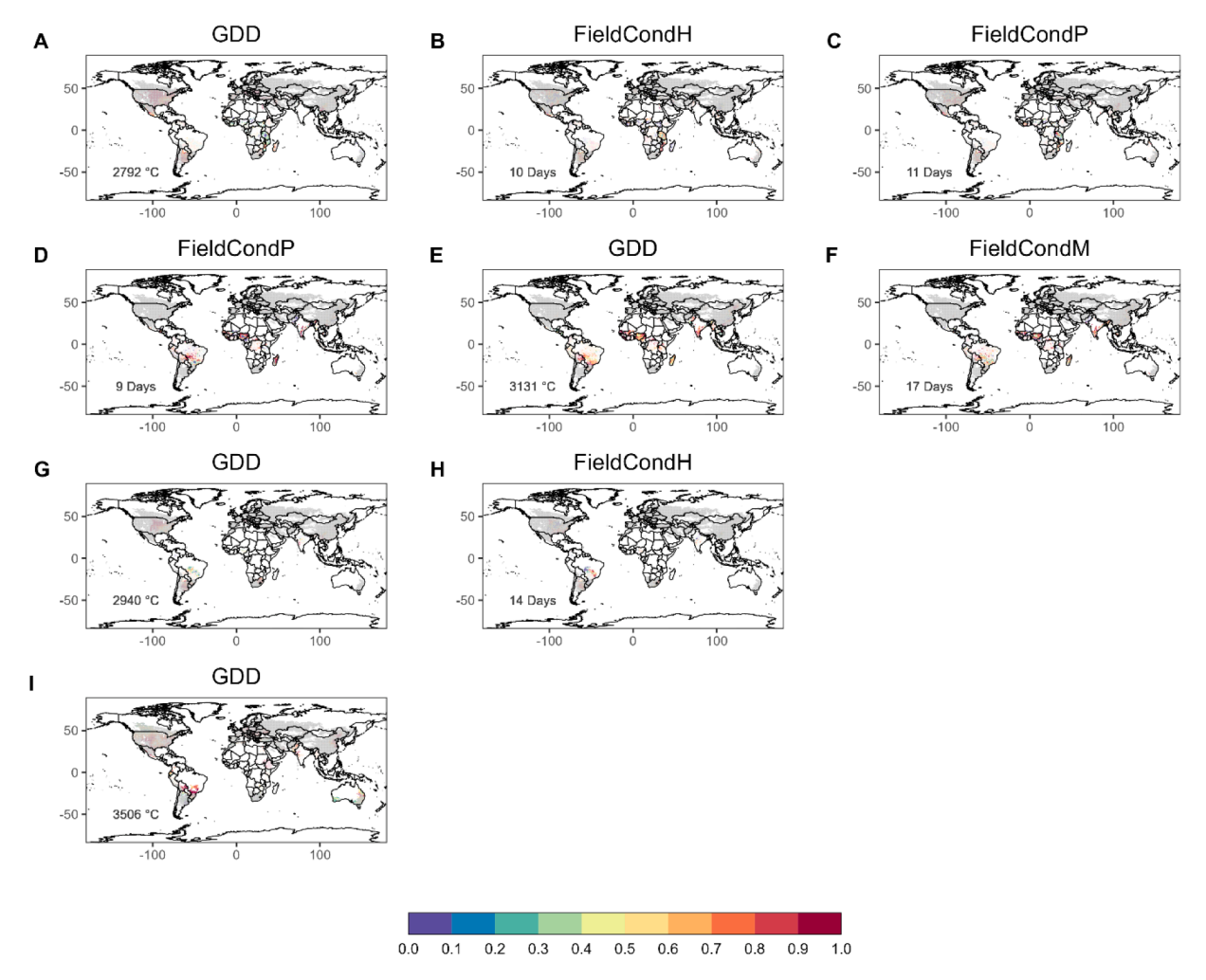


Fig. 8. The most influential agroclimatic indices in the tropic region on global croplands experiencing failures during extreme years for maize 2012 (A-C), rice 2002 (D-F), soy 2012 (G-H), and wheat 2002 (I) (from top row to bottom row). The color shows the percentile value for each pixel; the text shows the spatial average of actual values. Grey areas are the temperate region.

damages due to extreme drought (Li et al., 2019; Mangani et al., 2018). However, this study provides regional thresholds for GDD and Precip that can be used to inform stakeholders and may act as the foundations for index-based programs in regional markets where such analysis did not exist prior. It is also worth noting that HeatDay, as an extreme temperature index, is of relatively lower importance compared to GDD (Fig. 4). This is potentially a result of high thresholds (Table 1; reflecting heat tolerance) not being exceeded for extended periods in the growing season or during the vital reproductive period (Challinor et al., 2016; Hatfield and Prueger, 2015; Lobell et al., 2012; Luo, 2011). Research on future climate impacts of warming shows an increasing risk of increased production shocks reducing yield resulting in crop failure (Gaupp et al., 2019; Tigchelaar et al., 2018), and regions will become unfavorable for crop growth (Battisti and Naylor, 2009; Ceglar et al., 2019). Increasing temperature trends may result in more frequently surpassed current crop temperature thresholds, elevating the importance of *HeatDay*.

Besides *GDD* and *Precip*, this study also identified several influential indices that have been neglected in previous studies, including *FallFrost*, *SpFrost*, and optimal field conditions. Spring and fall frost dates are important in temperate regions. A *SpFrost* can harm sensitive young vegetation affecting its growth through the season (Pulatov et al., 2015; Sánchez et al., 2014; Wolfe et al., 2018). A severe *FallFrost* can prevent grain from reaching maturity, affecting seed quality and viability (DeVries et al., 2007). Optimal field conditions reflect the number of suitable workdays during different seasons. More days of optimal field

conditions indicate drier soils, while fewer days indicate wet soils (Trnka et al., 2011). Too few days of optimal field conditions may suggest damp and warm conditions that can accelerate the likeliness of seed germination and fungal infections, reducing yield (Powell and Reinhard, 2016). It can also result in crop lodging; some crops may be harvested with the return of favorable field conditions with added cost inputs, reducing yield (Peltonen-Sainio et al., 2018). On the other extreme, too many days of field conditions suggest drought conditions resulting in increased probabilities of crop failures (Figs. 4 and 5). These impacts could be very different during planting (FieldCondP), mid-season (FieldCondM), or harvesting seasons (FieldCondH).

Agroclimatic trends are salient for understanding the changing risk of crop failure. We find varying degrees of *Precip* within regions and globally, largely agreeing with the previous findings of decreasing *Precip* trends in warm regions and increasing *Precip* trends in cool regions (Nguyen et al., 2018). Increasing trends of *GDD* are consistent with previous research highlighting an increasing trend in global temperature (Lobell et al., 2011). Increase and decreases in *GDD* affect the phenology of crops. Increases in *GDD* hasten crop development leading to maturity being reached earlier resulting in less yield, while lower *GDD* slows growth making the crop more susceptible to pests, frost, and other factors (Alexandrov and Hoogenboom, 2000; Asseng et al., 2013). Our results also suggest that *FrostDays* are decreasing, earlier *SpFrost*, later *FallFrost*, and lengthening the *GrowSeason*. Our global analysis results are consistent with previous regional studies in North America (Kukal

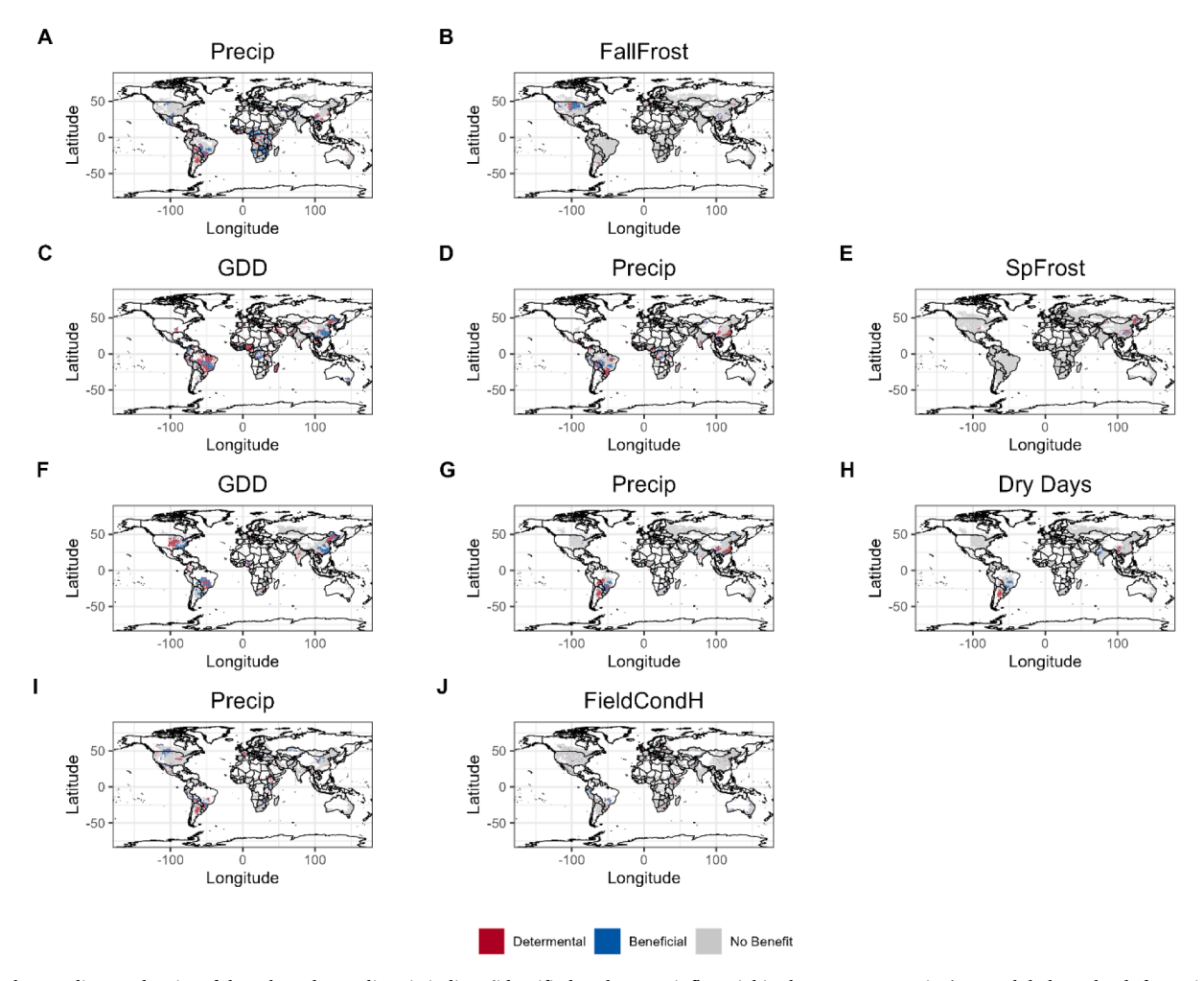


Fig. 9. The trending tendencies of the selected agroclimatic indices (identified as the most influential in the temperate region) over global croplands for maize (A-B), rice (C-E), soy (F-H), and wheat (I-J) (from top row to bottom row). The red color signifies that the current trends are trending toward more detrimental conditions (decreasing the distance between the agroclimate mean and the agroclimate condition when failures occurred), the bule color signifies that the current trends are trending toward more beneficial conditions (increasing, the distance between the agroclimate mean and the agroclimate condition when failures occurred) the grey color indicates regions where the agroclimate indices trend was not significant.

and Irmak, 2018) and Europe (Trnka et al., 2011). A lengthening of the growing season can result in more pest generations per season and northward migration, while warming of winter temperatures can result in pest overwintering (Wolfe et al., 2018). Together these impacts will result in the need for novel pest and disease control to reduce the impact to crop yields. Few studies have examined suitable field conditions regionally or globally. In East-Southeast Scotland, (Matthews et al., 2008), find an increase in dry soils; however, we find no significant trends at the same locations. We do find field conditions in tropical regions experience significant increasing or decreasing trends on nearly 30% of the cropland (Fig. 6). While optimal field conditions are commonly used to determine when producers can get into the field and prevent soil compaction and degradation, changes in field conditions may increase crop failure probabilities through delayed planting and harvesting due to wet conditions decreasing favorable field days (Peltonen-Sainio et al., 2018; Trnka et al., 2011). Delayed planting may result in unfavorable heat stress during the reproductive period, and delayed harvest can leave crops in the fields, decreasing the quality of the seed (Powell and Reinhard, 2016). Increases in favorable field condition days indicate drier conditions, increasing crop failure probability affecting crops similarly as decrease in Precip. Besides that, field conditions may be confounded with other factors such as previous growing season conditions, monsoons, and dry seasons that frequent tropical regions (Asharaf et al., 2012; Bapuji Rao et al., 2014; Swami

et al., 2018; Zachariah et al., 2020). Continual trends in either direction can result in increases to crop failure probability and agroclimate indices that may be toward beneficial conditions (Fig. 9 and 10) currently, they may or may not provide the same benefit in the future.

The findings from this study may inform climate adaptations in agriculture, such as crop failure early warning, breeding, and strategic planning of agricultural infrastructure and best management practices. We recognize that several agroclimatic variables are not included in this study, such as evapotranspiration and solar radiation, which may play an important role in determining crop failures. While our analysis is based on state-of-the-art datasets, it is subject to uncertainties from the crop, and climate data originating from satellite remote sensing, observations, and model approximations, particularly for regions with sparse ground observations. We also recognize that seasonal averaged variables can reduce apparent contributions of indices at various times in the growing season such, as *Precip* and *HeatDay*.

5. Conclusions

In this study, we characterize synchronized global crop failures using remote sensing-based products, analyze their predictability and relationships with agroclimatic conditions using machine learning, and identify trends of the most significant agroclimatic indices over global croplands. To our knowledge, this work is the first global-scale study

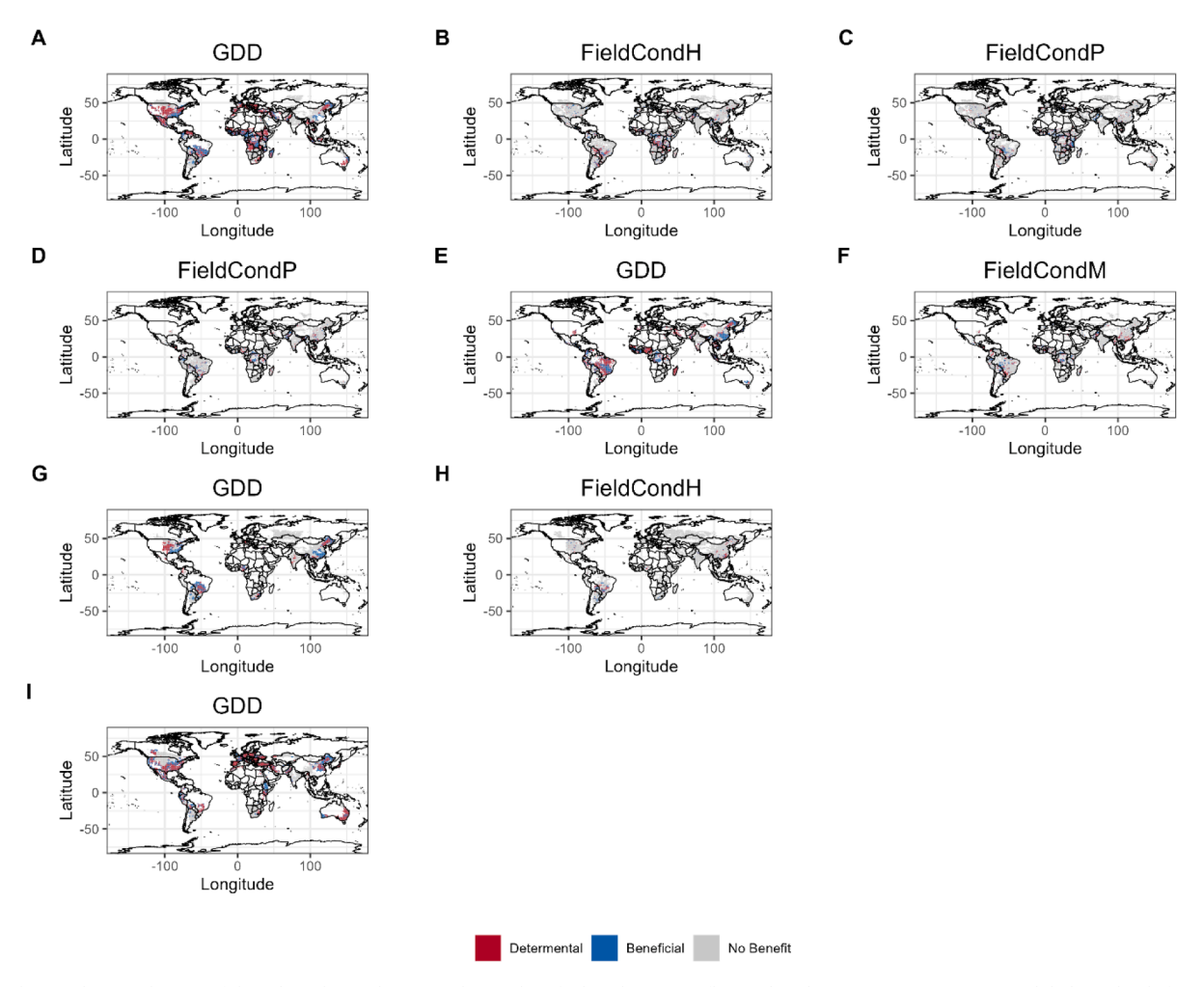


Fig. 10. The trending tendencies of the selected agroclimatic indices (identified as the most influential in the temperate region) over global croplands for maize (A-C), rice (D-G), soy (G-H), and wheat (I) (from top row to bottom row). The red color signifies that the current trends are trending toward more detrimental conditions (decreasing the distance between the agroclimate mean and the agroclimate condition when failures occurred), the bule color signifies that the current trends are trending toward more beneficial conditions (increasing, the distance between the agroclimate mean and the agroclimate condition when failures occurred) the grey color indicates regions where the agroclimate indices trend was not significant.

that considers 11 agroclimatic indices with strong agricultural significance and stakeholder interests, many of which were neglected in previous global studies. In addition, developing a machine learning-based approach to predicting and analyzing the crop failure is rarely investigated in previous studies. By analyzing the remote sensing-based crop yield data from 1981 to 2016, we found that the most extensive synchronous global crop failure events occurred in 2002 for maize and wheat, 2007 for soy, and 2004 for rice, when around 40% of global cropland experienced synchronous failures. Several regions were identified as contributing more to global crop failures than their contributions to global croplands, including East Asia and Sub-Sahara Africa for maize, East Asia and South and Southeast Asia for rice, Temperate South America for soy, and Europe and the Mediterranean and Sub-Sahara Africa for wheat. Machine learning models accurately predicted the occurrence of crop failures in different regions using agroclimatic indices, which are potentially useful for crop failure early warning. The models also reveal the most influential agroclimatic indices, including Precip, FallFrost, GDD, SpFrost, DryDays, and FieldCondH in the temperate region, and GDD, FieldCondH, FieldCondP, FieldCondM in the tropics. They show notable, non-linear responsive relationships with crop failures, with favorable conditions related to lowest failure probability differed by crops and regions, while deficient or excessive conditions both lead to dramatic increase in crop failures. These indices have mostly been experiencing significant trends on more than one-fourth of the temperate or tropical croplands from 1982 to 2016, with the trends in the temperature-based indices being more pronounced than in the moisture-based indices. The moisture-based trends are mostly increasing towards wetter conditions while relatively variable in space. The temperature-based indices are consistently increasing, shifting towards the conditions of extreme crop failure years for both temperature and tropic regions. Understanding what has the most influence on crop failure in a region has several advantages. The knowledge from this research can help develop early warning systems of crop failures, improving early distributions and allocations of food security aid before conditions worsen. Using thresholds of the most influential agroclimatic indices will improve index-based crop insurance in regions not currently implementing insurance, thus allowing producers to improve and grow their cropping practices and prepare and adapt to future climates with fewer livelihood concerns.

Declaration of Competing Interest

The authors declare that they have no known competing financial interests or personal relationships that could have appeared to influence the work reported in this paper.

Data availability

Data will be made available on request.

Acknowledgments

Research support provided through the NSF Research Traineeship Program (DGE-1922687), NSF CAREER Award (EAR-2144293), and the Hatch program of the USDA National Institute of Food and Agriculture (NIFA) (Accession No. 1012578). We acknowledge the Auburn University Easley Cluster for support of this work.

Supplementary materials

Supplementary material associated with this article can be found, in the online version, at doi:10.1016/j.agrformet.2023.109620.

References

- Alexandrov, V.A., Hoogenboom, G., 2000. Vulnerability and adaptation assessments of agricultural crops under climate change in the Southeastern USA. Theor. Appl. Climatol. 67, 45–63. https://doi.org/10.1007/s007040070015.
- Anandhi, A., Perumal, S., Gowda, P.H., Knapp, M., Hutchinson, S., Harrington, J., Murray, L., Kirkham, M.B., Rice, C.W., 2013. Long-term spatial and temporal trends in frost indices in Kansas, USA. Clim. Change 120, 169–181. https://doi.org/ 10.1007/s10584-013-0794-4.
- Anderson, W.B., Seager, R., Baethgen, W., Cane, M., You, L., 2019. Synchronous crop failures and climate-forced production variability. Sci. Adv. 5 https://doi.org/ 10.1126/sciady.aaw1976.
- Asharaf, S., Dobler, A., Ahrens, B., 2012. Soil moisture–precipitation feedback processes in the Indian summer monsoon season. J. Hydrometeorol. 13, 1461–1474. https://doi.org/10.1175/JHM-D-12-06.1.
- Asseng, S., Ewert, F., Martre, P., Rötter, R.P., Lobell, D.B., Cammarano, D., Kimball, B.A., Ottman, M.J., Wall, G.W., White, J.W., Reynolds, M.P., Alderman, P.D., Prasad, P.V. V., Aggarwal, P.K., Anothai, J., Basso, B., Biernath, C., Challinor, A.J., De Sanctis, G., Doltra, J., Fereres, E., Garcia-Vila, M., Gayler, S., Hoogenboom, G., Hunt, L.A., Izaurralde, R.C., Jabloun, M., Jones, C.D., Kersebaum, K.C., Koehler, A.K., Müller, C., Naresh Kumar, S., Nendel, C., O'leary, G., Olesen, J.E., Palosuo, T., Priesack, E., Eyshi Rezaei, E., Ruane, A.C., Semenov, M.A., Shcherbak, I., Stöckle, C., Stratonovitch, P., Streck, T., Supit, I., Tao, F., Thorburn, P.J., Waha, K., Wang, E., Wallach, D., Wolf, J., Zhao, Z., Zhu, Y., 2015. Rising temperatures reduce global wheat production. Nat. Clim. Chang. 5, 143–147. https://doi.org/10.1038/nclimate2470.
- Asseng, S., Ewert, F., Rosenzweig, C., Jones, J.W., Hatfield, J.L., Ruane, A.C., Boote, K.J., Thorburn, P.J., Rötter, R.P., Cammarano, D., Brisson, N., Basso, B., Martre, P., Aggarwal, P.K., Angulo, C., Bertuzzi, P., Biernath, C., Challinor, A.J., Doltra, J., Gayler, S., Goldberg, R., Grant, R., Heng, L., Hooker, J., Hunt, L.A., Ingwersen, J., Izaurralde, R.C., Kersebaum, K.C., Müller, C., Naresh Kumar, S., Nendel, C., O'Leary, G., Olesen, J.E., Osborne, T.M., Palosuo, T., Priesack, E., Ripoche, D., Semenov, M.A., Shcherbak, I., Steduto, P., Stöckle, C., Stratonovitch, P., Streck, T., Supit, I., Tao, F., Travasso, M., Waha, K., Wallach, D., White, J.W., Williams, J.R., Wolf, J., 2013. Uncertainty in simulating wheat yields under climate change. Nat. Clim. Chang. 3 (9 3), 827–832. https://doi.org/10.1038/nclimate1916, 2013.
- Bapuji Rao, B., Santhibhushan Chowdary, P., Sandeep, V.M., Rao, V.U.M., Venkateswarlu, B., 2014. Rising minimum temperature trends over India in recent decades: Implications for agricultural production. Glob. Planet Chang. 117, 1–8. https://doi.org/10.1016/J.GLOPLACHA.2014.03.001.
- Battisti, D.S., Naylor, R.L., 2009. Historical warnings of future food insecurity with unprecedented seasonal heat. Science (1979) 323, 240–244. https://doi.org/ 10.1126/SCIENCE.1164363.
- Bollero, G.A., Bullock, D.G., Hollinger, S.E., 1996. Soil temperature and planting date effects on corn yield, leaf area, and plant development. Agron. J. 88, 385. https://doi.org/10.2134/agronj1996.00021962008800030005x.
- Breiman, L., 2001. Random forests. Mach. Learn. 45, 5–32. https://doi.org/10.1023/A: 1010933404324.
- Bren D'Amour, C., Wenz, L., Kalkuhl, M., Christoph Steckel, J., Creutzig, F., 2016. Teleconnected food supply shocks. Environ. Res. Lett. 11, 035007 https://doi.org/ 10.1088/1748-9326/11/3/035007.
- Brown, I., 2013. Influence of seasonal weather and climate variability on crop yields in Scotland. Int. J. Biometeorol. 57, 605–614. https://doi.org/10.1007/s00484-012-0588-9.
- Çakir, R., 2004. Effect of water stress at different development stages on vegetative and reproductive growth of corn. Field Crops Res. 89, 1–16. https://doi.org/10.1016/j. fcr.2004.01.005.
- Ceglar, A., Turco, M., Toreti, A., Doblas-Reyes, F.J., 2017. Linking crop yield anomalies to large-scale atmospheric circulation in Europe. Agric. For. Meteorol. 240-241, 35–45. https://doi.org/10.1016/j.agrformet.2017.03.019.

- Ceglar, A., Zampieri, M., Toreti, A., Dentener, F., 2019. Observed northward migration of agro-climate zones in Europe will further accelerate under climate change. Earth. Future 7, 1088–1101. https://doi.org/10.1029/2019EF001178.
- Challinor, A.J., Koehler, A.K., Ramirez-Villegas, J., Whitfield, S., Das, B., 2016. Current warming will reduce yields unless maize breeding and seed systems adapt immediately. Nat. Clim. Chang. 6, 954–958. https://doi.org/10.1038/nclimate3061.
- Cooper, G., McGechan, M.B., Vinten, A.J.A., 1997. The influence of a changed climate on soil workability and available workdays in Scotland. J. Agricult. Eng. Res. 68, 253–269. https://doi.org/10.1006/jaer.1997.0204.
- Cottrell, R.S., Nash, K.L., Halpern, B.S., Remenyi, T.A., Corney, S.P., Fleming, A., Fulton, E.A., Hornborg, S., Johne, A., Watson, R.A., Blanchard, J.L., 2019. Food production shocks across land and sea. Nat. Sustain. 2, 130–137. https://doi.org/10.1038/s41893-018-0210-1
- DeVries, M., Goggi, A.S., Moore, K.J., 2007. Determining seed performance of frost-damaged maize seed lots. Crop Sci. 47, 2089–2097. https://doi.org/10.2135/CROPSCI2007.01.0005
- Erenstein, O., Chamberlin, J., Sonder, K., 2021. Estimating the global number and distribution of maize and wheat farms. Glob. Food Sec. 30, 100558 https://doi.org/ 10.1016/J.GFS.2021.100558.
- FAO, 2021. Food and Agriculture Data [WWW Document]. URL http://www.fao. org/faostat/en/#home (accessed 7.9.21).
- FAO, IFAD, UNICEF, WFP, WHO, 2021. The State of Food Security and Nutrition in the World 2021. Transforming food systems for food security, improved nutrition and affordable healthy diets for all. FAO, IFAD, UNICEF, WFP and WHO, Rome, Italy. https://doi.org/10.4060/ca9692en.
- Finger, R., 2013. Investigating the performance of different estimation techniques for crop yield data analysis in crop insurance applications. Agricult. Econ. 44, 217–230. https://doi.org/10.1111/agec.12005.
- Gaupp, F., Hall, J., Hochrainer-stigler, S., Dadson, S., 2020. Changing risks of simultaneous global breadbasket failure. Nat. Clim. Chang. 10, 54–57. https://doi. org/10.1038/s41558-019-0600-z.
- Gaupp, F., Hall, J., Mitchell, D., Dadson, S., 2019. Increasing risks of multiple breadbasket failure under 1.5 and 2°C global warming. Agric. Syst. 175, 34–45. https://doi.org/10.1016/j.agsy.2019.05.010.
- Goulart, H.M.D., Van Der Wiel, K., Folberth, C., Balkovic, J., Van Den Hurk, B., 2021. Storylines of weather-induced crop failure events under climate change. Earth Syst. Dynam 12, 1503–1527. https://doi.org/10.5194/esd-12-1503-2021.
- Gowda, P.H., Steiner, J.L., Olson, C., Boggess, M., Farrigan, T., Grusak, M.A., 2018. Chapter 10: Agriculture and Rural Communities. Impacts, Risks, and Adaptation in the United States: The Fourth National Climate Assessment, Volume II, Impacts, Risks, and Adaptation in the United States: Fourth National Climate Assessment. U.S. Global Change Research Program, Washington, DC. https://doi.org/10.7930/ NCA4.2018.CH10.
- Hatfield, J.L., Antle, J., Garrett, K.A., Izaurralde, R.C., Mader, T., Marshall, E., Nearing, M., Philip Robertson, G., Ziska, L., 2020. Indicators of climate change in agricultural systems. Clim. Change 163, 1719–1732. https://doi.org/10.1007/ s10584-018-2222-2.
- Hatfield, J.L., Prueger, J.H., 2015. Temperature extremes: Effect on plant growth and development. Weather Clim. Extrem. 10, 4–10. https://doi.org/10.1016/j. wace.2015.08.001.
- Iizumi, T., 2019. Global dataset of historical yields v1.2 and v1.3 aligned version. PANGAEA. https://doi.org/10.1594/PANGAEA.909132.
- Iizumi, T., Ramankutty, N., 2016. Changes in yield variability of major crops for 1981-2010 explained by climate change. Environ. Res. Lett. 11 https://doi.org/10.1088/ 1748-9326/11/3/034003
- Iizumi, T., Sakai, T., 2020. The global dataset of historical yields for major crops 1981–2016. Sci. Data 7, 1–7. https://doi.org/10.1038/s41597-020-0433-7.
- Jackson, N.D., Konar, M., Debaere, P., Sheffield, J., 2021. Crop-specific exposure to extreme temperature and moisture for the globe for the last half century. Environ. Res. Lett. 16 https://doi.org/10.1088/1748-9326/abf8e0.
- Jägermeyr, J., Müller, C., Ruane, A.C., Elliott, J., Balkovic, J., Castillo, O., Faye, B., Foster, I., Folberth, C., Franke, J.A., Fuchs, K., Guarin, J.R., Heinke, J., Hoogenboom, G., Iizumi, T., Jain, A.K., Kelly, D., Khabarov, N., Lange, S., Lin, T.-S., Liu, W., Mialyk, O., Minoli, S., Moyer, E.J., Okada, M., Phillips, M., Porter, C., Rabin, S.S., Scheer, C., Schneider, J.M., Schyns, J.F., Skalsky, R., Smerald, A., Stella, T., Stephens, H., Webber, H., Zabel, F., Rosenzweig, C., 2021. Climate impacts on global agriculture emerge earlier in new generation of climate and crop models. Nat. Food 2. https://doi.org/10.1038/s43016-021-00400-y.
- Jeong, J.H., Resop, J.P., Mueller, N.D., Fleisher, D.H., Yun, K., Butler, E.E., Timlin, D.J., Shim, K.M., Gerber, J.S., Reddy, V.R., Kim, S.H., 2016. Random forests for global and regional crop yield predictions. PLoS One 11. https://doi.org/10.1371/journal. pone.0156571.
- Kamara, A.Y., Menkir, A., Badu-Apraku, B., Ibikunle, O., 2003. The influence of drought stress on growth, yield and yield components of selected maize genotypes. J. Agric. Sci. 141, 43–50. https://doi.org/10.1017/S0021859603003423.
- Kukal, M.S., Irmak, S., 2018. U.S. agro-climate in 20th century: growing degree days, first and last frost, growing season length, and impacts on crop yields. Sci. Rep. 8 https://doi.org/10.1038/s41598-018-25212-2.
- Lau, W.K.M., Kim, K.-M., Lau, W.K.M., Kim, K.-M., 2012. The 2010 Pakistan flood and russian heat wave: teleconnection of hydrometeorological extremes. J. Hydrometeorol. 13, 392–403. https://doi.org/10.1175/JHM-D-11-016.1.
- Leng, G., Hall, J.W., 2020. Predicting spatial and temporal variability in crop yields: An inter-comparison of machine learning, regression and process-based models. Environ. Res. Lett. 15, 44027. https://doi.org/10.1088/1748-9326/ab7b24.

- Li, Y., Guan, K., Schnitkey, G.D., DeLucia, E., Peng, B., 2019. Excessive rainfall leads to maize yield loss of a comparable magnitude to extreme drought in the United States. Glob. Chang. Biol. 25, 2325–2337. https://doi.org/10.1111/gcb.14628.
- Liaw, A., Wiener, M., 2018. Classification and Regression by randomForest, 2. R News, pp. 18–22. https://doi.org/10.1177/154405910408300516.
- Lobell, D.B., Field, C.B., 2007. Global scale climate-crop yield relationships and the impacts of recent warming. Environ. Res. Lett. 2 https://doi.org/10.1088/1748-9326/2/1/014002.
- Lobell, D.B., Hammer, G.L., McLean, G., Messina, C., Roberts, M.J., Schlenker, W., 2013. The critical role of extreme heat for maize production in the United States. Nat. Clim. Chang. 3, 497–501. https://doi.org/10.1038/nclimate1832.
- Lobell, D.B., Schlenker, W., Costa-Roberts, J., 2011. Climate trends and global crop production since 1980. Science (1979) 333, 616–621. https://doi.org/10.1126/ science.1204531.
- Lobell, D.B., Sibley, A., Ivan Ortiz-Monasterio, J., 2012. Extreme heat effects on wheat senescence in India. Nat. Clim. Chang. 2, 186–189. https://doi.org/10.1038/ nclimate1356.
- Luo, Q., 2011. Temperature thresholds and crop production: a review. Clim. Change 109, 583–598. https://doi.org/10.1007/s10584-011-0028-6.
- Mangani, R., Tesfamariam, E.H., Bellocchi, G., Hassen, A., 2018. Growth, development, leaf gaseous exchange, and grain yield response of maize cultivars to drought and flooding stress. Sustainability 10, 3492. https://doi.org/10.3390/su10103492.
- Martens, B., Miralles, D.G., Lievens, H., van der Schalie, R., De Jeu, R.A.M.M., Fernández-Prieto, D., Beck, H.E., Dorigo, W.A., Verhoest, N.E.C.C., 2017. GLEAM v3: Satellite-based land evaporation and root-zone soil moisture. Geosci. Model. Dev. 10, 1903–1925. https://doi.org/10.5194/gmd-10-1903-2017.
- Matthews, K.B., Rivington, M., Buchan, K., Miller, D., Bellocchi, G., 2008. Characterising the agro-meteorological implications of climate change scenarios for land management stakeholders. Clim. Res. 37, 59–75. https://doi.org/10.3354/cr00751.
- Mehrabi, Z., Ramankutty, N., 2019. Synchronized failure of global crop production. Nat. Ecol. Evol. 3, 780–786. https://doi.org/10.1038/s41559-019-0862-x.
- Miralles, D.G., Holmes, T.R.H., De Jeu, R.A.M., Gash, J.H., Meesters, A.G.C.A., Dolman, A.J., 2011. Global land-surface evaporation estimated from satellite-based observations. Hydrol. Earth Syst. Sci. 15, 453–469. https://doi.org/10.5194/hess-15-453-2011.
- Molnar, C., 2019. Interpretable Machine Learning, 1st ed.
- Monfreda, C., Ramankutty, N., Foley, J.A., 2008. Farming the planet: 2. Geographic distribution of crop areas, yields, physiological types, and net primary production in the year 2000. Glob. Biogeochem. Cycles 22, 1–19. https://doi.org/10.1029/2007GB002947.
- Monier, E., Xu, L., Snyder, R., 2016. Uncertainty in future agro-climate projections in the United States and benefits of greenhouse gas mitigation. Environ. Res. Lett. 11 https://doi.org/10.1088/1748-9326/11/5/055001.
- Muchow, R.C., Sinclair, T.R., Bennett, J.M., 1990. Temperature and solar radiation effects on potential maize yield across locations. Agron. J. 82, 338–343. https://doi. org/10.2134/agronj1990.00021962008200020033x.
- Nguyen, P., Thorstensen, A., Sorooshian, S., Hsu, K., AghaKouchak, A., Ashouri, H., Tran, H., Braithwaite, D., 2018. Global precipitation trends across spatial scales using satellite observations. Bull. Am. Meteorol. Soc. 99, 689–697. https://doi.org/ 10.1175/RAMS.D-17-0065.1
- Nóia Júnior, R.D.S., Martre, P., Finger, R., Van Der Velde, M., Ben-Ari, T., Ewert, F., Webber, H., Ruane, A.C., Asseng, S., 2021. Extreme lows of wheat production in Brazil. Environ. Res. Lett. 16, 104025 https://doi.org/10.1088/1748-9326/AC26F3.
- Ortiz-Bobea, A., Ault, T.R., Carrillo, C.M., Chambers, R.G., Lobell, D.B., 2021.

 Anthropogenic climate change has slowed global agricultural productivity growth.

 Nat. Clim. Chang. 11, 306–312. https://doi.org/10.1038/s41558-021-01000-1.
- Peltonen-Sainio, P., Jauhiainen, L., Hakala, K., 2011. Crop responses to temperature and precipitation according to long-term multi-location trials at high-latitude conditions. J. Agricult. Sci. 149, 49–62. https://doi.org/10.1017/S0021859610000791.
- Peltonen-Sainio, P., Palosuo, T., Ruosteenoja, K., Jauhiainen, L., Ojanen, H., 2018. Warming autumns at high latitudes of Europe: an opportunity to lose or gain in cereal production? Reg. Environ. Change 18, 1453–1465. https://doi.org/10.1007/S10113-017-1275-5/FIGURES/10.
- Powell, J.P., Reinhard, S., 2016. Measuring the effects of extreme weather events on yields. Weath. Clim. Extrem. 12, 69–79. https://doi.org/10.1016/j. wace.2016.02.003.
- Pulatov, B., Linderson, M.L., Hall, K., Jönsson, A.M., 2015. Modeling climate change impact on potato crop phenology, and risk of frost damage and heat stress in northern Europe. Agric. For. Meteorol. 214-215, 281–292. https://doi.org/10.1016/ J.AGRFORMET.2015.08.266.

- Puma, M.J., Bose, S., Chon, S.Y., Cook, B.I., 2015. Assessing the evolving fragility of the global food system. Environ. Res. Lett. 10, 024007 https://doi.org/10.1088/1748-9326/10/2/024007
- Ray, D.K., Gerber, J.S., Macdonald, G.K., West, P.C., 2015. Climate variation explains a third of global crop yield variability. Nat. Commun. 6, 1–9. https://doi.org/ 10.1038/ncomms6989
- Sacks, W.J., Deryng, D., Foley, J.A., Ramankutty, N., 2010. Crop planting dates: an analysis of global patterns. Glob. Ecol. Biogeogr. 19, 607–620. https://doi.org/ 10.1111/j.1466-8238.2010.00551.x.
- Sánchez, B., Rasmussen, A., Porter, J.R., 2014. Temperatures and the growth and development of maize and rice: a review. Glob. Chang. Biol. 20, 408–417. https:// doi.org/10.1111/gcb.12389.
- Schierhorn, F., Hofmann, M., Gagalyuk, T., Ostapchuk, I., Müller, D., 2021. Machine learning reveals complex effects of climatic means and weather extremes on wheat yields during different plant developmental stages. Clim. Change 169, 1–19. https:// doi.org/10.1007/S10584-021-03272-0/FIGURES/5.
- Schillerberg, T.A., Tian, D., 2020. Changes of crop failure risks in the United States associated with large-scale climate oscillations in the Atlantic and Pacific Oceans. Environ. Res. Lett. 15 https://doi.org/10.1088/1748-9326/ab82cd.
- Schillerberg, T.A., Tian, D., Miao, R., 2019. Spatiotemporal patterns of maize and winter wheat yields in the United States: Predictability and impact from climate oscillations. Agric. For. Meteorol. 275, 208–222. https://doi.org/10.1016/j. agrformet 2019 05 019
- Schlenker, W., Roberts, M.J., 2009. Nonlinear temperature effects indicate severe damages to U.S. crop yields under climate change. Proc. Natl. Acad. Sci. U. S. A. 106, 15594–15598. https://doi.org/10.1073/pnas.0906865106.
- Song, H., Li, Y., Zhou, L., Xu, Z., Zhou, G., 2018. Maize leaf functional responses to drought episode and rewatering. Agric. For. Meteorol. 249, 57–70. https://doi.org/ 10.1016/j.agrformet.2017.11.023.
- Swami, D., Dave, P., Parthasarathy, D., 2018. Agricultural susceptibility to monsoon variability: A district level analysis of Maharashtra, India. Sci. Tot. Environ. 619-620, 559–577. https://doi.org/10.1016/J.SCITOTENV.2017.10.328.
- Tack, J., Barkley, A., Hendricks, N., 2017. Irrigation offsets wheat yield reductions from warming temperatures. Environ. Res. Lett. 12, 114027 https://doi.org/10.1088/ 1748-9326/aa8d27.
- Terando, A., Keller, K., Easterling, W.E., 2012. Probabilistic projections of agro-climate indices in North America. J. Geophys. Res. Atmosph. 117, 1–16. https://doi.org/ 10.1029/2012/ID017436.
- Tigchelaar, M., Battisti, D.S., Naylor, R.L., Ray, D.K., 2018. Future warming increases probability of globally synchronized maize production shocks. Proc. Natl. Acad. Sci. U. S. A. 115, 6644–6649. https://doi.org/10.1073/pnas.1718031115.
- Trnka, M., Olesen, J.E., Kersebaum, K.C., Skjelvåg, A.O., Eitzinger, J., Seguin, B.,
 Peltonen-Sainio, P., Rötter, R.P., Iglesias, A., Orlandini, S., Dubrovský, M.,
 Hlavinka, P., Balek, J., Eckersten, H., Cloppet, E., Calanca, P., Gobin, A., Vučetić, V.,
 Nejedlik, P., Kumar, S., Lalic, B., Mestre, A., Rossi, F., Kozyra, J., Alexandrov, V.,
 Semerádová, D., Žalud, Z., 2011. Agroclimatic conditions in Europe under climate change. Glob. Chang. Biol. 17, 2298–2318. https://doi.org/10.1111/j.1365-2486.2011.02396.x
- USDA Foreign Agricultural Service, 2021. Oilseeds: World Markets and Trade.
- Vogel, E., Donat, M.G., Alexander, L.V., Meinshausen, M., Ray, D.K., Karoly, D., Meinshausen, N., Frieler, K., 2019. The effects of climate extremes on global agricultural yields. Environ. Res. Lett. 14 https://doi.org/10.1088/1748-9326/ ab154b
- Wegren, S.K., 2011. Food security and Russia's 2010 drought. Eurasian Geogr. Econ. 52, 140–156. https://doi.org/10.2747/1539-7216.52.1.140.
- Wilks, D.S., 2011. Statistical Methods in the Atmospheric Sciences, 3rd ed. International Geophysics Series. Academic Press.
- Wolfe, D.W., DeGaetano, A.T., Peck, G.M., Carey, M., Ziska, L.H., Lea-Cox, J., Kemanian, A.R., Hoffmann, M.P., Hollinger, D.Y., 2018. Unique challenges and opportunities for northeastern US crop production in a changing climate. Clim. Change 146, 231–245. https://doi.org/10.1007/s10584-017-2109-7.
- Zachariah, M., Mondal, A., Das, M., Achutarao, K.M., Ghosh, S., 2020. On the role of rainfall deficits and cropping choices in loss of agricultural yield in Marathwada, India. Environ. Res. Lett. 15, 094029 https://doi.org/10.1088/1748-9326/AB93FC.
- Zaveri, E., Lobell, D.B., 2019. The role of irrigation in changing wheat yields and heat sensitivity in India. Nat. Commun. 10, 1–7. https://doi.org/10.1038/s41467-019-12183-9.
- Zhu, X., Troy, T.J., 2018. Agriculturally relevant climate extremes and their trends in the world's major growing regions. Earth. Future 6, 656–672. https://doi.org/10.1002/ 2017FF000687